Numerical modeling of the oceanic S_1 tide for Earth rotation studies

EGU General Assembly, 12 – 17 April 2015, Vienna

Michael Schindelegger[1], David Einšpigel[2]
[1] Vienna University of Technology, Austria
[2] School of Cosmic Physics, Dublin Institute for Advanced Studies, Ireland

Summary

Diurnal S_1 oceanic oscillations induced by atmospheric pressure loading elicit small but measurable perturbations of universal time, pole position, and the prograde annual component of nutation. Deducing accurate estimates of these signals is a delicate challenge that involves the determination of oceanic angular momentum (OAM) values from free-running forward integrations of the shallow water equations. This study employs a simple barotropic ocean model to assess the dependence of the OAM vector in the diurnal band on three key model components: (1) the formulation of dissipative processes; (2) the choice of barometric tidal forcing; and (3) the treatment of ocean self-attraction and loading (SAL). OAM values appear to vary considerably with the specified air tide but are far less sensitive to how open ocean dissipation and the SAL tidal forcing are formulated. When superimposed on the diurnal angular momentum of the atmosphere and converted to excitation estimates, our hydrodynamic S_1 solutions yield a reasonably good account of the prograde annual nutation as observed with geodetic VLBI (Very Long Baseline Interferometry).

Variables & Symbols

- $\boldsymbol{u}$ ... *velocity vector*
- ζ ... *tidal elevation*
- H ... *water depth*
- f ... *Coriolis parameter*
- $\hat{k}$ ... *vertical unit vector*
- ω ... *tidal frequency*
- g ... *gravitational accel.*
- ρ ... *seawater density*

Theoretical buoyancy frequencies for IT drag:

$$N_b = 5.24 \cdot 10^{-3} e^{-H/1300}$$

$$\bar{N} = 1300 \cdot 5.24 \cdot 10^{-3} \cdot (1 - e^{-H/1300})/H$$

S_1 and Earth's nutation

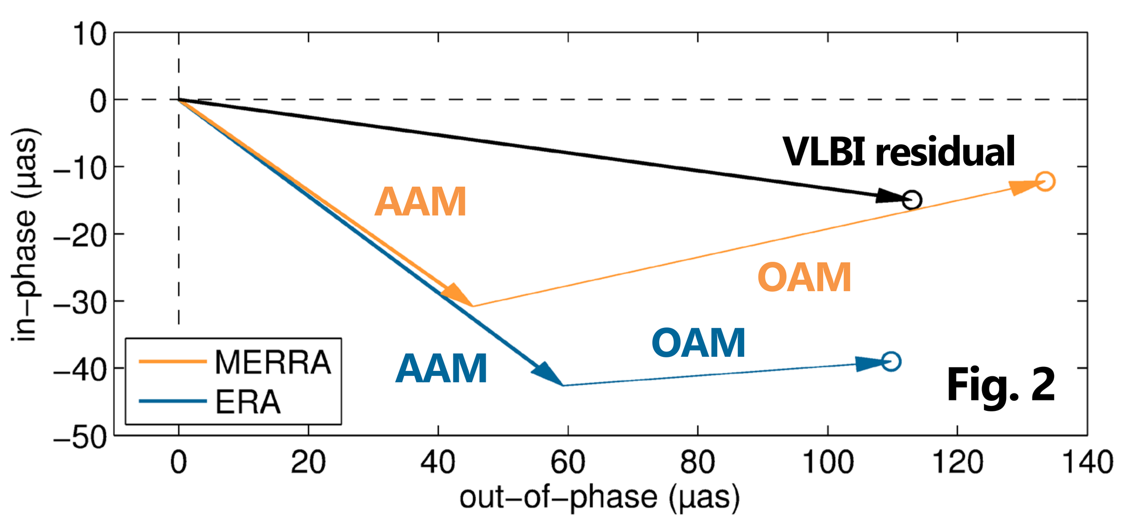

Fig. 2

When viewed from inertial space, the diurnal-period S_1 wave in the atmosphere and oceans perturbs Earth's prograde annual nutation at a level of 100 µas but existing geophysical model estimates of this effect have deviated significantly from its observational evidence in geodetic VLBI data. Using the present global numerical model results from MERRA, ERA, and a consistently forced barotropic ocean model, our integral excitation estimates agree, however, within about 20 – 30 µas, with the empirical VLBI residual (**Fig. 2**).

Acknowledgement: We thank the Austrian Science Fund FWF for financial support of this study under project ASPIRE (I1479) .

Der Wissenschaftsfonds.

Global barotropic tide model

We adapt the time-stepping model of Einšpigel & Martinec (2015) for simulations forced by selected equilibrium tides ζ_{EQ} (M_2, O_1) and atmospheric S_1 pressure P. The 2D momentum equations read:

$$\frac{\partial \boldsymbol{u}}{\partial t} + f\hat{k} \times \boldsymbol{u} + \frac{3 \cdot 10^{-3} \|\boldsymbol{u}\| \boldsymbol{u}}{H + \zeta} =$$

$$= -g\nabla\left(\zeta - \zeta_{EQ} - \boxed{\underbrace{\zeta_{SAL}}_{3} - \underbrace{P/\rho g}_{2}\Big) - \underbrace{\mathcal{F}}_{1}}$$

Key components: 3 2 1

Configuration:
- 1/3° x 1/3° Arakawa C-grid, ETOPO1 bathymetry
- Time step of 24 seconds, 12-day spin up

1 Open ocean dissipation

Our time-stepping model overestimates tidal heights and OAM unless substantial drag in the abyssal ocean is present. For practical purposes, the accuracy of surface elevations can be controlled by a tunable but inordinately high horizontal eddy viscosity ($2.2 \cdot 10^5\ m^2/s$ in this study). A physically more plausible scheme is to parametrize the sub-grid scale conversion of barotropic energy to internal tides (IT) over rough topography by aid of a linear drag term:

$$\mathcal{F} = C_{IT} \frac{\boldsymbol{u}}{H + \zeta}, \quad C_{IT} = 100H(\nabla H)^2 \frac{N_b \bar{N}}{8\pi^2 \omega}$$

Zaron & Egbert (2006)

Using this parametrization, RMS elevation discrepancies with respect to altimetric tidal solutions are 6.8 cm (M_2) and 1.5 cm (O_1) but somewhat larger differences are obtained if we tune by viscosity. In terms of S_1 OAM, the two schemes differ by a few percent (**Table 1**).

2 Meteorological forcing

Two 40-day simulations deploying internal tide drag and an iterative SAL correction were performed using S_1 surface pressure tide climatologies deduced from:

- **MERRA** (Modern-Era Retrospective Analysis for Research and Applications): 3-hourly "assimilated states", 1.25° grid, 2004–2013
- **ERA**-Interim (Reanalysis of the European Centre for Medium-Range Weather Forecasts): 6-hourly analysis, 1° grid, 2001–2010

The resulting S_1 tidal elevation charts (**Fig. 1a** and **1b**) reveal sizable dissimilarities in amplitude and phase, cf. e.g. the lower-magnitude ERA-solution in middle and higher latitudes. Accordingly, large disparities are found between individual OAM components based on MERRA- and ERA-forcing (**Table 1**).

3 Self-attraction and loading

In numerical tide models, gravitational and loading feedback effects on tidal dynamics are accounted for either approximately – by the simple scaling relationship $\zeta_{SAL} = \beta\zeta$ – or more rigorously through iteration, i.e. successive model runs where each simulation uses knowledge of the tidal heights from the previous run (ζ_{prev}). Our implementation follows *Arbic et al.* (2004) and requires offline convolution with the SAL Green's function G_{SAL} in between two runs.

$$\zeta_{SAL} = \rho a^2 \iint \zeta_{prev} G_{SAL}\, dS - \underbrace{\beta(\zeta - \zeta_{prev})}_{\text{"Memory term" enforcing convergence}}$$

Provided a careful choice of β (0.12 for diurnal tides), OAM values from the scalar approximation are very close to those from the iterative solution (**Table 1**).

Table 1: Global angular momentum integrals of the S_1 ocean tide deduced from different model runs. Amplitudes in units of $10^{23}\ \mathrm{kgm^2s^{-1}}$ and cotidal phases relative to Greenwich noon; cf. *Ray & Egbert* (2004) which serves as a reference for the present study.

Atm. Model		MERRA			MERRA	ERA	Ray & Egbert
Dissipation $\mathcal{F}$			IT Drag		Viscosity	IT Drag	None
SAL formalism		Scalar ($\beta = 0.12$)	1 iteration	2 iterations	2 iterations	2 iterations	4 iterations
Mass	x	0.22 (209°)	0.28 (204°)	0.29 (209°)	0.40 (218°)	1.49 (155°)	0.82 (158°)
	y	3.76 (320°)	3.78 (319°)	3.77 (319°)	3.88 (317°)	2.47 (290°)	2.90 (306°)
	z	3.37 (239°)	3.35 (236°)	3.33 (236°)	3.29 (235°)	2.22 (225°)	2.42 (219°)
Motion	x	2.25 (5°)	2.20 (6°)	2.19 (5°)	2.23 (4°)	1.52 (323°)	1.72 (14°)
	y	2.54 (193°)	2.57 (192°)	2.59 (192°)	2.72 (188°)	2.68 (172°)	1.62 (226°)
	z	1.27 (254°)	1.12 (249°)	1.12 (255°)	1.19 (249°)	2.06 (282°)	2.57 (271°)

S_1 ocean tide charts

Fig. 1a: Amplitudes (top, in mm) and Greenwich phase lags (bottom, in deg) of S_1 as computed from our hydrodynamic model using forcing from MERRA.

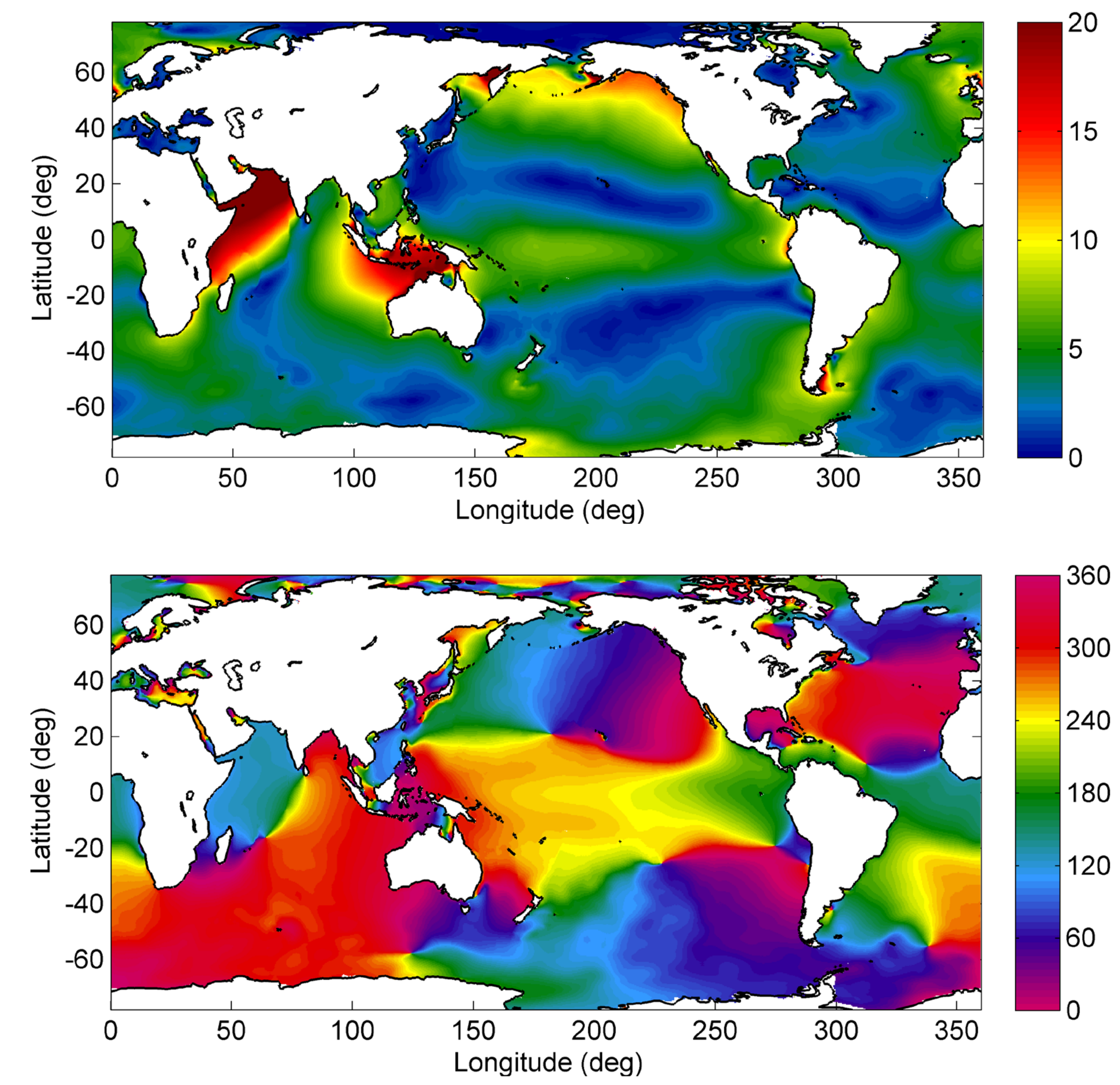

Fig. 1b: Same as Fig. 1a but with forcing from ERA.

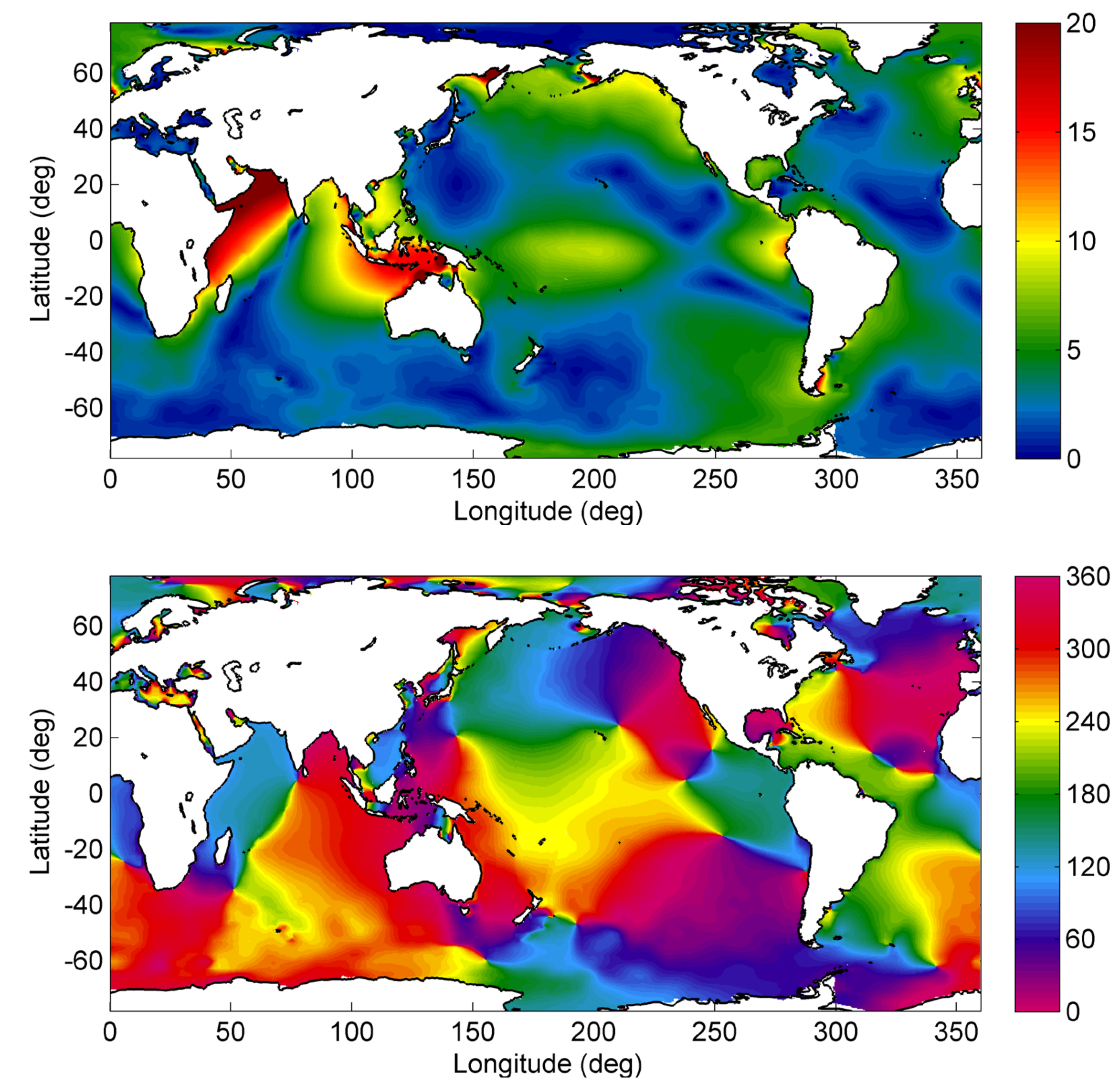

References

Arbic, B. et al. (2004). The accuracy of surface elevations in forward global barotropic and baroclinic tide models. *Deep-Sea Res. Pt. II*, 51, 3069–3101.

Einšpigel, D. and Martinec, Z. (2015). The new derivation of the shallow water equations in geographical coordinates and their application to a global barotropic ocean model, submitted to *Ocean Modelling*.

Ray, R. and Egbert, G. (2004). The global S_1 tide. *J. Phys. Oceanogr.*, 34, 1922–1935.

Zaron, E. and Egbert, G. (2006). Estimating open-ocean barotropic tidal dissipation: The Hawaiian Ridge. *J. Phys. Oceanogr.*, 36, 1019–1035.